Wiley
Advances in High Energy Physics
Volume 2025, Article ID 6941883, 14 pages
https://doi.org/10.1155/ahep/6941883

WILEY

Research Article

Interplay Between M_W, $\Omega_{\mathrm{CDM}}h^2$, and $(g-2)_\mu$ in Flavor Symmetry–Based Supersymmetric Models

Sajid Israr,[1] **Mario E. Gómez**,[2] **Muhammad Rehman**,[1] **and Yasir Arafat**[3]

[1]*Department of Physics, Comsats University Islamabad, Islamabad, Pakistan*
[2]*Department of Applied Physics, University of Huelva, Huelva, Spain*
[3]*Center for High Energy Physics, University of the Punjab, Lahore, Pakistan*

Correspondence should be addressed to Muhammad Rehman; m.rehman@comsats.edu.pk

Received 18 October 2024; Accepted 23 May 2025

Academic Editor: Torsten Asselmeyer-Maluga

We study the phenomenological implications of the minimal supersymmetric standard model (MSSM) augmented by a nonabelian flavor symmetry labeled as sMSSM. Incorporating this flavor symmetry allows for a significant reduction in the original plethora of free parameters present in the MSSM, ultimately reducing them down to just seven in sMSSM. This reduction of free parameters is not achieved through ad hoc assumptions like in the constrained MSSM (CMSSM); rather, it is grounded in theoretical considerations. Our work focuses on exploring the interplay between the W boson mass (M_W) predictions, the cold dark matter (CDM) relic abundance ($\Omega_{\mathrm{CDM}}h^2$), and the $(g-2)_\mu$ anomaly. We identified correlations among the theoretical parameters arising from this interplay, which can be complemented by experimental constraints such as the Higgs boson mass, B-physics observables, and charge and color breaking minima. Additionally, our investigations show that the $(g-2)_\mu$ discrepancy and the Planck bounds on $\Omega_{CDM}h^2$ can be addressed within the sMSSM but only in a very narrow region of the parameter space.

1. Introduction

The minimal supersymmetric standard model (MSSM) [1–6] is widely recognized as one of the most popular theories beyond the standard model (SM) [7–10]. However, due to its extensive set of more than 105 free parameters, making meaningful phenomenological predictions becomes challenging. To address this issue, researchers have explored different approaches to reduce the number of free parameters. One such approach is the constrained MSSM (CMSSM) [11], where specific assumptions are employed to simplify the model and bring down the number of free parameters to just five. It is important to note that these simplifications are not based on theoretical considerations but rather rely on ad hoc assumptions.

While the CMSSM offers a highly idealized version, it is worth mentioning that the realistic supersymmetric (SUSY) models may encompass additional complexities and nonuniversalities in the soft SUSY-breaking (SSB) parameters. These intricacies can significantly impact collider searches, cosmology, and other experimental and theoretical investigations. Moreover, the experimental landscape does not currently favor the CMSSM, as recent findings from the CMS and ATLAS experiments have imposed rigorous limitations on the CMSSM parameter space [12]. As a result, researchers are actively investigating alternative models, including the phenomenological MSSM and models based on symmetry principles. An example of an alternative model to the CMSSM is the flavor symmetry–based minimal supersymmetric standard model (sMSSM) [13], which incorporates a nonabelian flavor symmetry denoted as H. The number of free parameters in the sMSSM remains at a manageable level, with just two additional parameters compared to the CMSSM.

Recently, the CDF collaboration has unveiled an intriguing indicator of potential new physics through its assessment

of the mass of the W boson [14] displaying a significant deviation of approximately 7σ with the SM predictions [15]. Apart from this discrepancy, there has also been considerable attention given to the long-standing anomaly in the $(g-2)_\mu$ value. The most recent assessment conducted by the muon $g-2$ collaboration at Fermilab [16, 17], when combined with the earlier findings from the Brookhaven E821 experiment [18], reveals a deviation of 5.1σ from the SM prediction [19].

Numerous studies in the existing literature have focused on exploring the phenomenological aspects of the sMSSM, including the $(g-2)_\mu$ anomaly and predictions for $\Omega_{\mathrm{CDM}}h^2$ [20–22]. In light of the recent CDF results and their implications for the M_W world average, predictions for the W boson mass have also become crucial. The interplay between $\Omega_{\mathrm{CDM}}h^2$, $(g-2)_\mu$, and M_W can provide valuable insights for the MSSM [23].

This work involves computing $\Omega_{\mathrm{CDM}}h^2$, $(g-2)_\mu$, and M_W within the sMSSM frameworks. The main objective is to determine if the $(g-2)_\mu$ and M_W anomalies, along with $\Omega_{\mathrm{CDM}}h^2$, can be explained within the sMSSM. Our analysis is conducted through the utilization of SARAH [24–28], SPheno [29], micrOMEGAs [30–32], and SARAH Scan and Plot (SSP) [33] setup. Initially, we employed SARAH to generate the MSSM source code for SPheno, facilitating subsequent tasks such as spectrum generation and the computation of low-energy observables like B-physics observables, $\Delta\alpha_\mu$, and the mass of the W boson using SPheno. Moreover, the output from SPheno was employed as input for micrOMEGAs to evaluate the relic density of dark matter.

The paper is organized as follows: first, we present the main features of the sMSSM in Section 2. Elaboration on the specifics of the calculations regarding low-energy observables like M_W and new physics contributions to $(g-2)_\mu$ namely the $\Delta\alpha_\mu$ can be found in Section 3. The computational details and numerical results are presented in Section 4. Our conclusions can be found in Section 5.

2. sMSSM

The MSSM represents the most basic form of SUSY that can be constructed using the particle content of the SM. The overall configuration for the SSB parameters is given by [1–6]

$$\begin{aligned}-\mathscr{L}_{\mathrm{soft}} = {} & \left(m_{\tilde{Q}}^2\right)_i^j \tilde{q}_L^{\dagger i}\tilde{q}_{Lj} + \left(m_{\tilde{u}}^2\right)_j^i \tilde{u}_{Ri}^* \tilde{u}_R^j + \left(m_{\tilde{d}}^2\right)_j^i \tilde{d}_{Ri}^* \tilde{d}_R^j \\ & + \left(m_{\tilde{L}}^2\right)_i^j \tilde{l}_L^{\dagger i}\tilde{l}_{Lj} + \left(m_{\tilde{e}}^2\right)_j^i \tilde{e}_{Ri}^* \tilde{e}_R^j + \tilde{m}_1^2 h_1^\dagger h_1 + \tilde{m}_2^2 h_2^\dagger h_2 \\ & + \left(B_\mu h_1 h_2 + \mathrm{h.c.}\right) + \Big(A_d^{ij} h_1 \tilde{d}_{Ri}^* \tilde{q}_{Lj} + A_u^{ij} h_2 \tilde{u}_{Ri}^* \tilde{q}_{Lj} \\ & + A_l^{ij} h_1 \tilde{e}_{Ri}^* \tilde{l}_{Lj} + \frac{1}{2} M_1 \tilde{B}_L \tilde{B}_L + \frac{1}{2} M_2 \tilde{W}_L^a \tilde{W}_L^a \\ & + \frac{1}{2} M_3 \tilde{G}^a \tilde{G}^a + \mathrm{h.c.}\Big).\end{aligned} \tag{1}$$

Here, the symbols $m_{\tilde{Q}}^2$ and $m_{\tilde{L}}^2$ represent 3×3 matrices in the family space, with indices i and j denoting generations, encapsulating the SSB masses for the left-handed squark doublets $\tilde{q}_L$ and slepton doublets $\tilde{l}_L$ associated with the SU(2) symmetry. Similarly, the matrices $m_{\tilde{u}}^2$, $m_{\tilde{d}}^2$, and $m_{\tilde{e}}^2$ incorporate the soft masses for the right-handed up-type squarks $\tilde{u}_R$, down-type squarks $\tilde{d}_R$, and charged sleptons $\tilde{e}_R$, which are SU(2) singlets. The matrices A_u, A_d, and A_l are also 3×3 matrices, signifying the trilinear couplings concerning up-type squarks, down-type squarks, and charged sleptons, respectively. The parameter μ corresponds to the Higgs mixing, while $\tilde{m}_1$, $\tilde{m}_2$, and B_μ stand as the SSB factors are related to the Higgs sector. Within this context, h_1 and h_2 denote the two Higgs doublets. Lastly, the terms M_1, M_2, and M_3 define the mass parameters of the bino, wino, and gluino, respectively.

Equation (1) encompasses over 105 free parameters, rendering the generation of viable phenomenological predictions within the context of the MSSM nearly impractical. However, this extensive list of parameters is significantly pruned down to a mere 5 within the CMSSM. This simplification is achieved by making the assumption that scalar masses are equivalent at the GUT scale, and likewise, the gaugino masses are equal as well. The foundation of the CMSSM finds its roots in minimal supergravity [34–36]. However, this structure does not stem from theoretical considerations; instead, it relies on some ad hoc assumptions. Additionally, results from experiments at the LHC have constrained the parameter range of the CMSSM to a minimum extent.

A category of SUSY models where the form of the SSB Lagrangian is determined solely by considerations of symmetry have been developed to overcome the limitations posed by the CMSSM. This framework is known as the sMSSM which is defined with a SSB Lagrangian that satisfies two essential symmetry conditions. Firstly, the parameters are consistent with a grand unified symmetry such as SO(10). Secondly, a nonabelian flavor symmetry H operates on the three generations of particles, effectively suppressing excessive flavor-changing neutral currents (FCNCs) mediated by the SUSY particles.

Explicit examples of these models are constructed using flavor symmetries such as gauged $\mathrm{SU}(2)_H$ and $\mathrm{SO}(3)_H$, where the three generations of particles transform as $\mathbf{2}+\mathbf{1}$ and $\mathbf{3}$ representations, respectively. In the framework of $\mathrm{SU}(2)_H$, there is a straightforward solution for suppressing flavor-violating D-terms based on an interchange symmetry and the $\mathrm{SO}(3)_H$ symmetry framework naturally avoid the D-term issues. Moreover, within the framework of H, it is sufficient for only the first two generations to constitute a shared multiplet to address the SUSY flavor problem. Meanwhile, the third family can be treated as a singlet. Therefore, both $\mathbf{2}+\mathbf{1}$ assignment of fermion fields under H as well as $\mathbf{3}$ assignment are equally valid.

Compatibility with SO(10) unified symmetry has major advantages from the standpoint of SSB. By dropping the number of soft masses for sfermions from 15 associated with the SM gauge symmetry (matching to the 15 chiral multiplets of the SM) to just three, it significantly lowers the

number of free parameters for these particles. In addition, it offers a symmetry-based justification for the gaugino masses' unification, decreasing the free parameters from three in the SM to one. There are two more free parameters in sMSSM compared to CMSSM making the total up to seven. These are

$$\left\{m_{0_{1,2}}, m_{0_3}, M_{1/2}, A_0, , \mu, m_A\right\},$$

where $m_{0_{1,2}}$ represents the SSB mass parameter for the first two families of sfermions, m_{0_3} for the third generation, $M_{1/2}$ for the SSB gaugino mass, and A_0 for the SSB trilinear coupling. The parameters μ and M_A represent the ratio of the vacuum expectation values of the two Higgs doublets, bilinear Higgs mixing term and the mass of the CP-odd Higgs boson, respectively.

3. Calculation of Low-Energy Observables

3.1. SUSY Contributions to the Mass of the W Boson. The CDF collaboration has disclosed a fascinating signal hinting at the possibility of new physics beyond the SM as they examined the mass of the W boson. Their measurement yields a value [14]:

$$M_W^{\mathrm{CDF}} = 80.4335 \pm 0.0094,$$

displaying a significant deviation of approximately 7σ from the prediction within the SM [15], where

$$M_W^{\mathrm{SM}} = 80.357 \pm 0.006.$$

Upon combining the previous results of the experiments like ATLAS and LHCb for M_W, the world average is determined as [37]

$$M_W^{\mathrm{avg}} = 80.4133 \pm 0.0080,$$

thereby resulting in a deviation of about 6.5σ. Despite thorough considerations of quantum corrections to the mass of the W boson (as discussed in Reference [38] and references therein), there still remains an outstanding discrepancy of approximately 5.1σ when compared to the SM prediction. In light of these findings, it becomes plausible to attribute this deviation from the SM to the potential influence of new physics beyond the SM.

The W boson mass is modified by the shifts in the electroweak parameter ρ according to

$$\Delta M_W \approx \frac{M_W}{2}\frac{c_w^2}{c_w^2 - s_w^2}\Delta\rho, \tag{2}$$

where c_W (s_W) are the cos (sin) of the Weinberg angle θ_W. The parameter $\Delta\rho$ can be calculated by the relation

$$\Delta\rho = \frac{\sum_Z^T(0)}{M_Z^2} - \frac{\sum_W^T(0)}{M_W^2} \tag{3}$$

where $\sum_{Z,W}^T(0)$ denote the unrenormalized transverse parts of the Z- and W-boson self-energies at zero momentum. The top and bottom quarks give the dominant contributions to the ρ in the SM which is given by

$$\rho = \frac{3G_\mu}{8\sqrt{2}\pi^2} F_0\left(m_b^2, m_t^2\right) \tag{4}$$

where G_μ represents the usual Fermi constant while m_b and m_t represent the masses of bottom and top quarks, respectively. $F_0(m_1^2, m_2^2)$ is defined as

$$F_0\left(m_1^2, m_2^2\right) = m_1^2 + m_2^2 - \frac{2m_1^2 m_2^2}{m_1^2 - m_2^2}\ \ln\ \frac{m_1^2}{m_2^2}. \tag{5}$$

In the SM, the contributions to ρ originate from the mass difference in one SU(2) doublet. The picture is more intricate in the MSSM [39–41]. Representative Feynman diagrams for the scalar quarks' contributions are shown in Figure 1. Here, only the squarks' contributions to ρ are shown. However, ρ also receive corrections from sleptons and other particles that exist within the MSSM framework. For our numerical evaluation, we have used SARAH-generated SPheno code to calculate the W boson mass which incorporate all these correction into account.

Contributions beyond one-loop have not been considered. For instance, two-loop SUSY contributions to $\Delta\rho$ are evaluated in Reference [42] where the reported values are typically one or more orders of magnitude smaller than one-loop contributions. Given the SUSY mass scale considered in the present work, we do not expect significant corrections from higher order contributions.

3.2. SUSY Contributions to $(g-2)_\mu$. There has been considerable attention given to the long-standing anomaly in the $(g-2)_\mu$ value. The most recent assessment conducted by the Run II and Run III of muon $g-2$ collaboration at Fermilab [16], when combined with the earlier findings from the same experiment [17] and Brookhaven E821 experiment [18], reveals a deviation of 5.1σ [43] from the SM prediction [19, 44]:

$$\Delta\alpha_\mu = \alpha_\mu^{exp} - \alpha_\mu^{SM} = (24.9 \pm 4.8) \times 10^{-10}. \tag{6}$$

This discrepancy can be solved by considering the MSSM contributions to $(g-2)_\mu$. The dominant MSSM contributions originate from the sleptons, chargino and neutralino loops and are shown in Figure 2.

The corrections from the Feynman diagrams shown in diag $(g-2)$ can be summarized as [45–49]

$$\begin{aligned}\Delta\alpha_\mu^{\mathrm{MSSM}} = \Delta\alpha_\mu^{\tilde{B}\tilde{\mu}_L\tilde{\mu}_R} + \Delta\alpha_\mu^{\left(\tilde{B}-\tilde{H}\right)\tilde{\mu}_L} + \Delta\alpha_\mu^{\left(\tilde{H}-\tilde{B}\right)\tilde{\mu}_R} \\ + \Delta\alpha_\mu^{\left(\tilde{H}-\tilde{W}\right)\tilde{\mu}_L} + \Delta\alpha_\mu^{\left(\tilde{W}-\tilde{H}\right)\tilde{\nu}_\mu}\end{aligned} \tag{7}$$

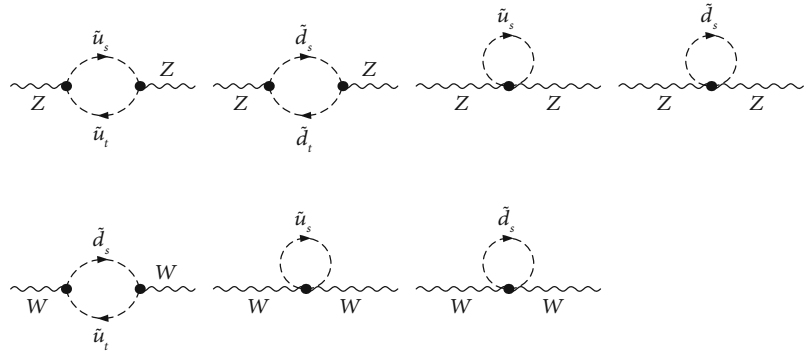

Figure 1: One-loop self-energy Feynman diagrams for Z and W bosons. $\tilde{u}_{s,t}$ and $\tilde{d}_{s,t}$ represent the six mass eigenstates of up-type and down-type scalar quarks, respectively.

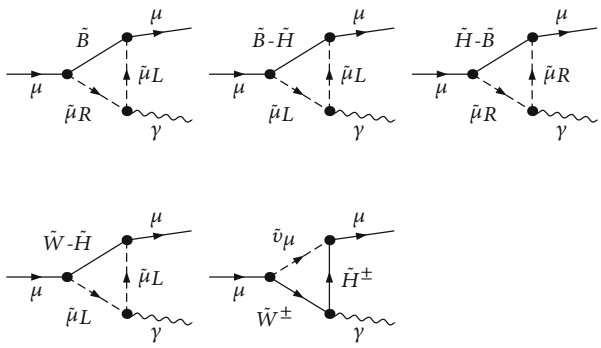

Figure 2: Feynman diagrams for dominant MSSM contributions to $(g-2)_\mu$ originating from different neutralino and chargino species. The diagrams shown as ($\tilde{B}$-$\tilde{H}$), ($\tilde{H}$-$\tilde{B}$), and ($\tilde{W}$-$\tilde{H}$) represent mixing between neutralino species.

where

$$\Delta\alpha_\mu^{\tilde{B}\tilde{\mu}_L\tilde{\mu}_R} = \frac{g_Y^2}{8\pi^2}\frac{m_\mu^2\mu}{M_1^3}F_b\left(\frac{m_{\tilde{\mu}_L}^2}{M_1^2},\frac{m_{\tilde{\mu}_R}^2}{M_1^2}\right) \tag{8}$$

$$\Delta\alpha_\mu^{(\tilde{H}-\tilde{B})\tilde{\mu}_R} = \frac{-g_Y^2}{8\pi^2}\frac{m_\mu^2 M_1\mu}{m_{\tilde{\mu}_R}^4}F_b\left(\frac{M_1^2}{m_{\tilde{\mu}_R}^2},\frac{\mu^2}{m_{\tilde{\mu}_R}^2}\right) \tag{9}$$

$$\Delta\alpha_\mu^{(\tilde{B}-\tilde{H})\tilde{\mu}_L} = \frac{g_Y^2}{16\pi^2}\frac{m_\mu^2 M_1\mu}{m_{\tilde{\mu}_L}^4}F_b\left(\frac{M_1^2}{m_{\tilde{\mu}_L}^2},\frac{\mu^2}{m_{\tilde{\mu}_L}^2}\right) \tag{10}$$

$$\Delta\alpha_\mu^{(\tilde{H}-\tilde{W})\tilde{\mu}_L} = \frac{-g^2}{16\pi^2}\frac{m_\mu^2 M_2\mu}{m_{\tilde{\mu}_L}^4}F_b\left(\frac{M_2^2}{m_{\tilde{\mu}_L}^2},\frac{\mu^2}{m_{\tilde{\mu}_L}^2}\right) \tag{11}$$

$$\Delta\alpha_\mu^{(\tilde{W}-\tilde{H})\tilde{\nu}_\mu} = \frac{g^2}{8\pi^2}\frac{m_\mu^2 M_2\mu}{m_{\tilde{\nu}_\mu}^4}F_a\left(\frac{M_2^2}{m_{\tilde{\nu}_\mu}^2},\frac{\mu^2}{m_{\tilde{\nu}_\mu}^2}\right) \tag{12}$$

with $F_a(x,y)$ and $F_b(x,y)$ defined as

$$F_a(x,y) = \frac{-1}{2(x-y)}\left(\frac{(x-1)(x-3)+2\ln x}{(x-1)^3} - \frac{(y-1)(y-3)+2\ln y}{(y-1)^3}\right),$$

$$F_b(x,y) = \frac{-1}{2(x-y)}\left(\frac{(x-1)(x+1)-2x\ln x}{(x-1)^3} - \frac{(y-1)(y+1)-2y\ln y}{(y-1)^3}\right).$$

As can be seen from Equations (8)–(12), all the contributions are proportional to μ; however, the value of μ is constrained by the vacuum stability bounds and electroweak symmetry breaking (EWSB).

In addition to the previously discussed one-loop corrections, two-loop corrections can also play a significant role in certain regions of the parameter space [50, 51]. Specifically, two-loop corrections to SM-like one-loop diagrams [52, 53] can be substantial in some cases but exhibit a decoupling behavior, diminishing as the masses of SUSY particles or heavy Higgs bosons increase. Given that our present analysis involves large SUSY masses, we do not anticipate significant corrections.

4. Numerical Results

4.1. Computational Strategy. The following is a brief description of our computation workflow. With the help of Mathematica package SARAH [24–28], we first created the MSSM source code for SPheno [29]. SPheno is a package that numerically calculates SUSY mass spectra, decay rates of particles, and various low energy observables like ρ and $\Delta\alpha_\mu$. Likewise, we generated the micrOMEGAs [30–32] source code using SARAH to incorporate the constraints from the dark matter observables into our analysis. These files are interfaced with SSP [33], which is a Mathematica package that facilitates parameter scanning and plotting. For the sMSSM framework, the following parameter set was used for random scans:

$$\begin{aligned} 0 \leq \quad & m_{0_{1,2}} \quad \leq 5\,\text{TeV} \\ 0 \leq \quad & m_{0_3} \quad \leq 15\,\text{TeV} \\ 0 \leq \quad & M_{1/2} \quad \leq 2\,\text{TeV} \\ -3 \leq \quad & A_0/m_{0_3} \quad \leq 3\,\text{TeV} \\ 0 \leq \quad & \mu \quad \leq 2\,\text{TeV} \\ 0 \leq \quad & M_A \quad \leq 10\,\text{TeV} \\ 1 \leq \quad & \tan\beta \quad \leq 60. \end{aligned}$$

These prescribed boundaries were applied at the GUT scale, with the exception of the parameters μ and M_A, which were instead defined at the SUSY scale. A private code written to calculate the charge and color breaking minima constraints (CCB) based on References [54, 55] was also implemented in the SSP package and data was generated in accordance with the following bounds on the low energy observables:

$$\begin{aligned} & M_h = 123 - 127\,\text{GeV}, \\ & m_{\tilde{g}} \geq 2.1\,\text{TeV}, \\ & 1.99 \times 10^{-9} \leq \text{BR}(B_s \longrightarrow \mu^+\mu^-) \leq 3.43 \times 10^{-9}\ (2\sigma), \\ & 3.02 \times 10^{-4} \leq \text{BR}(B \longrightarrow X_s\gamma) \leq 3.62 \times 10^{-4}\ (2\sigma), \\ & 0.115 \leq \Omega_{\text{CDM}}h^2 \leq 0.125(5\sigma). \end{aligned} \tag{13}$$

The current theoretical uncertainty in MSSM predictions for stands at approximately the 2 GeV level [56]. Hence, we have opted for a range of 123 GeV $\leq M_h \leq$ 127 GeV. Regarding M_W, we have selected the 2σ range of M_W^{avg}, while the values for $\text{BR}(B \longrightarrow X_s\gamma)$ and $\text{BR}(B_s \longrightarrow \mu^+\mu^-)$ have been chosen at the 2σ level of their experimentally measured value [15, 57]. The lower limit on Ω_{CDM} [58] may be disregarded as other particle species could also contribute to the DM relic abundance. Consequently, we exclusively consider points that align with the LSP neutralino relic density, ensuring it remains consistent with or lower than the Planck measurements. Nonetheless, we have examined the parameter space where both upper and lower limits could be satisfied.

4.2. Constraints and Correlation Between Input Parameters. In our effort to resolve the W boson mass anomaly, the $(g-2)_\mu$ discrepancy, and the constraints imposed by $\Omega_{\text{CDM}}h^2$ within the framework of the sMSSM, we meticulously examined the most appropriate parameter space. Our analysis revealed correlations between the input parameters and the various constraints on these parameters.

In Figure 3b, we present the sMSSM's predictions for M_h in the $M_{1/2} - m_{0_3}$ plane. The color bar indicates the value of M_h. Experimental limits on the masses of squarks and gluinos constrain the $M_{1/2}$ parameter to be greater than 800 Gev. It is also evident that is highly sensitive to m_{0_3} and increases with increasing m_{0_3}. However, no points are obtained for $m_{0_3} \lesssim 7$ TeV. This constraint primarily ensures that M_h falls within the 123–127 GeV range. To clarify further, Figure 3a shows M_h versus m_{0_3}, with the color bar indicating the value of $m_{0_{1,2}}$.

In Figure 4a, we show the correlation between μ, $m_{0_{1,2}}$, and $\tan\beta$. We observe that $m_{0_{1,2}}$ values increase with $\tan\beta$, with the highest $m_{0_{1,2}}$ values corresponding to extreme $\tan\beta$ values. Notably, there are no points for $\tan\beta < 10$ and $m_{0_{1,2}} < 3.5$ for $\tan\beta < 30$. Higher values of $m_{0_{1,2}}$ (above 3.5 TeV) are only possible for $\tan\beta > 30$. This is likely related to EWSB. In Figure 4b, the correlation between $m_{0_{1,2}}$, $\Delta\alpha_\mu^{\text{MSSM}}$, and μ is presented. As can be observed, the required values for $\Delta\alpha_\mu^{\text{MSSM}}$ can only be obtained for $m_{0_{1,2}} < 3$ TeV.

Figure 5 presents the sMSSM predictions for $\Delta\alpha_\mu^{\text{MSSM}}$ in the $m_{0_{1,2}} - m_{0_3}$ (Figure 5a) and $M_{1/2} - m_{0_{1,2}}$ (Figure 5b) planes. As shown, $\Delta\alpha_\mu^{\text{MSSM}}$ favors values of $m_{0_{1,2}}$ below 3 GeV. In summary, the experimental constraints on M_h and $m_{\tilde{g}}$, the upper limit on $\Omega_{\text{CDM}}h^2$, and the $(g-2)_\mu$ anomaly further narrow down the parameter space of the sMSSM to

$$\begin{aligned} 0 \leq \quad & m_{0_{1,2}} \quad \leq 3\,\text{TeV} \\ 7 \leq \quad & m_{0_3} \quad \leq 15\,\text{TeV} \\ 0.8 \leq \quad & M_{1/2} \quad \leq 2\,\text{TeV} \\ 0 \leq \quad & \mu \quad \leq 570\,\text{GeV} \end{aligned}$$

The constraints on $m_{0_{1,2}}$ and μ originate from considerations of $(g-2)_\mu$, while the constraints on m_{0_3} and $M_{1/2}$ are due to M_h and $m_{\tilde{g}}$, respectively.

4.3. $\Delta\alpha_\mu$ and $\Omega_{CDM}h^2$ in the sMSSM. In this section, we discuss the predictions for $\Omega_{\text{CDM}}h^2$ within the sMSSM and the resulting constraints imposed on the sMSSM parameter space by $\Omega_{\text{CDM}}h^2$. Generally, we found that points contributing significantly to M_W and satisfying the condition $\Omega_{\text{CDM}}h^2 \leq 0.125$ require a μ value below 1 TeV. For these points, the lightest supersymmetric particle (LSP) is a neutralino, which is a mixture of higgsino and bino components. To characterize the higgsino component of the LSP, we consider the lightest neutralino as follows:

$$\chi = N_{11}\tilde{B} + N_{12}\tilde{W} + N_{13}\tilde{H}_1 + N_{14}\tilde{H}_2. \tag{14}$$

We characterize the higgsino composition as $(N_{13}^2 + N_{14}^2) \times 100$. In Figure 6a,b, we show the higgsino component of the LSP versus $m_{\tilde{\chi}_1^0}$ (μ), with the color bar representing the value of $\Omega_{\text{CDM}}h^2$ and the orange points in Figure 6b represent locations where $\Delta\alpha_\mu^{\text{MSSM}}$ falls within the 2σ range required to address the $(g-2)_\mu$ discrepancy. It is evident that the higgsino component is significant for most of the displayed points. Additionally, we observe that $\Omega_{\text{CDM}}h^2$ increases as the

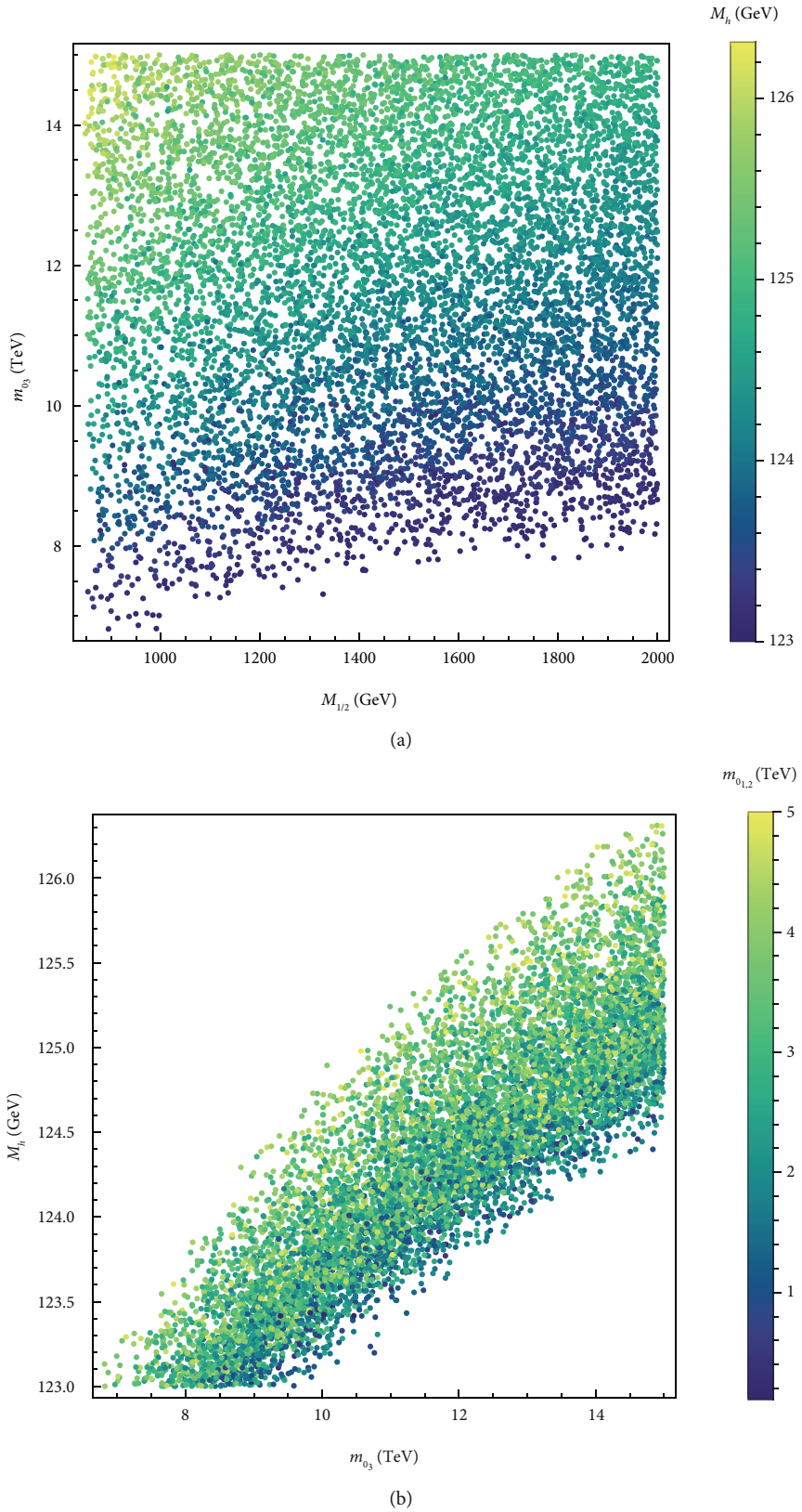

FIGURE 3: (a) sMSSM's predictions for M_h in the $M_{1/2} - m_{0_3}$ plane, with the color bar representing the value of M_h. (b) M_h versus m_{0_3}, with the color bar indicating the value of $m_{0_{1,2}}$.

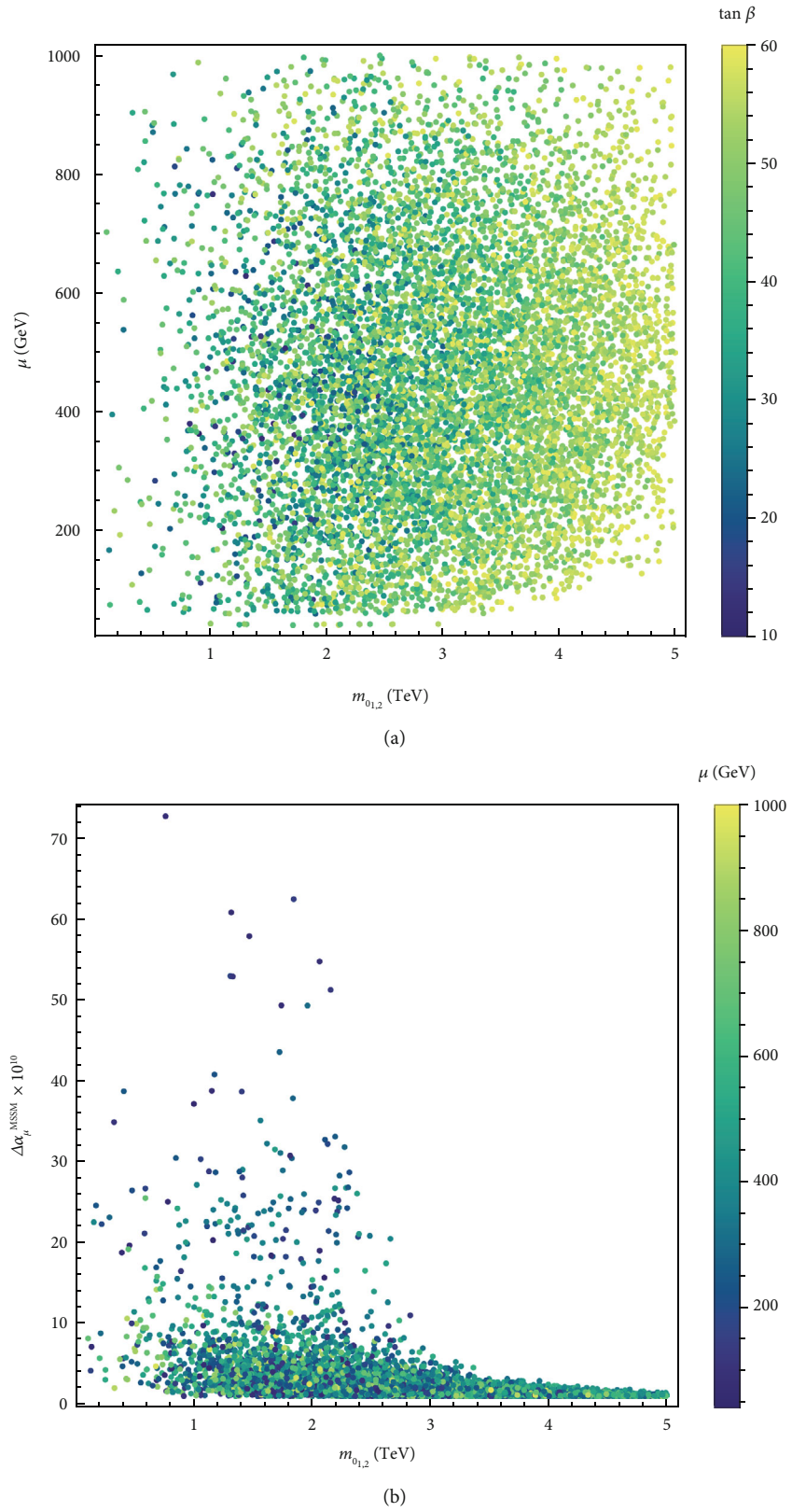

FIGURE 4: (a) The correlation between μ, $m_{0_{1,2}}$, and tan β, with the color bar indicating the value of tan β. (b) The correlation between $m_{0_{1,2}}$, $\Delta\alpha_\mu^{\mathrm{MSSM}}$, and μ, with the color bar representing the value of μ.

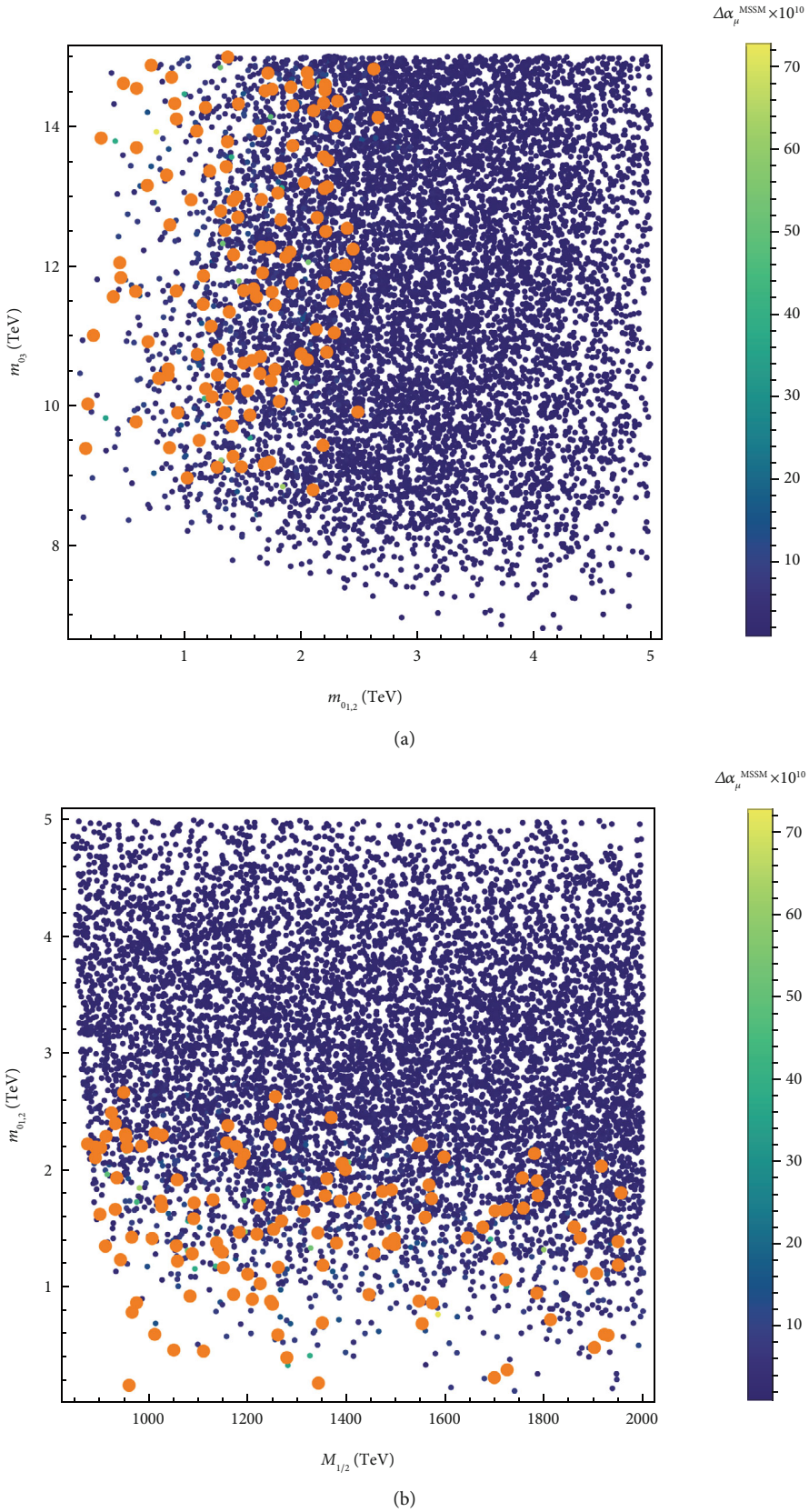

FIGURE 5: The sMSSM's predictions for $\Delta\alpha_\mu^{\text{MSSM}}$ in the (a) $m_{0_{1,2}} - m_{0_3}$ and (b) $M_{1/2} - m_{0_3}$ plane, with the color bar representing the value of $\Delta\alpha_\mu^{\text{MSSM}}$. The orange points in (a) represent locations where $\Delta\alpha_\mu^{\text{MSSM}}$ falls within the 2σ range required to address the $(g-2)_\mu$ discrepancy.

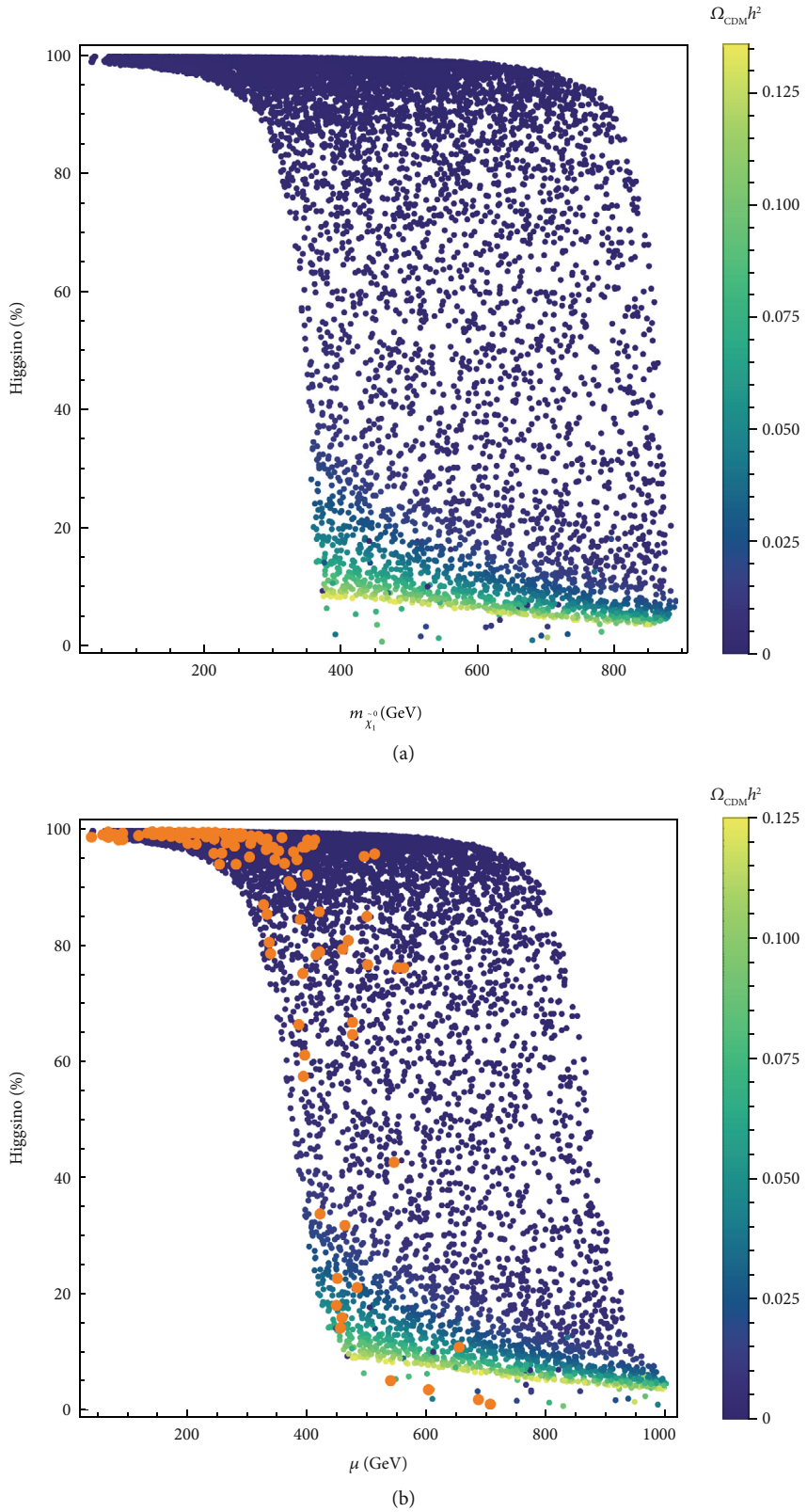

FIGURE 6: Higgsino percentage versus (a) $m_{\tilde{\chi}_1^0}$ and (b) μ, with the color bar indicating the value of $\Omega_{\mathrm{CDM}}h^2$. The orange points in (b) represent locations where $\Delta a_\mu^{\mathrm{MSSM}}$ falls within the 2σ range required to address the $(g-2)_\mu$ discrepancy.

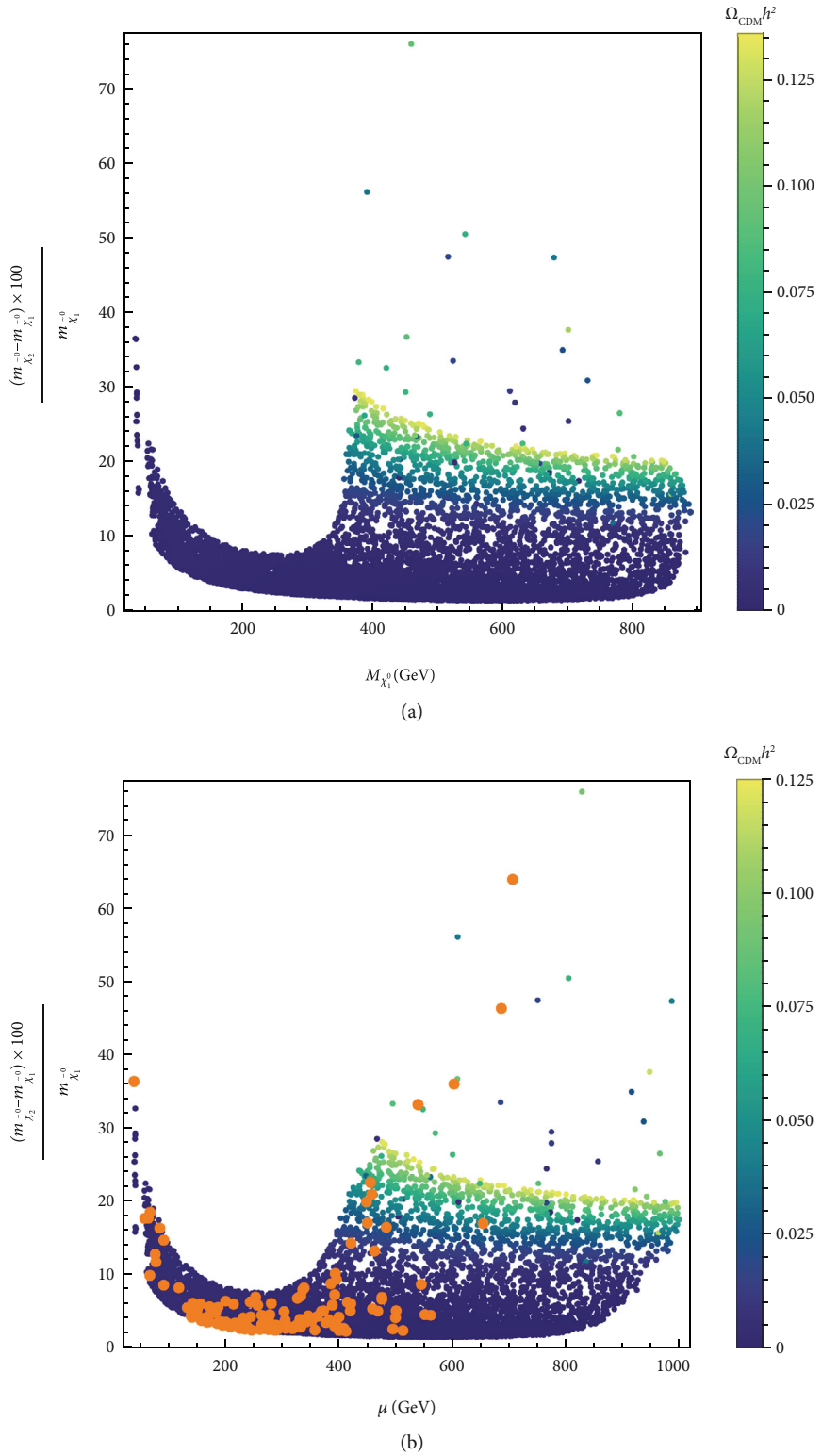

FIGURE 7: Relative ratio $(m_{\tilde{\chi}_2^0} - m_{\tilde{\chi}_1^0}) \times 100/m_{\tilde{\chi}_1^0}$ versus (a) $m_{\tilde{\chi}_1^0}$ and (b) μ while the color bar depicts the value of $\Omega_{\mathrm{CDM}}h^2$. The orange points in the right plot represent locations where $\Delta\alpha_\mu^{\mathrm{MSSM}}$ falls within the 2σ range required to address the $(g-2)_\mu$ discrepancy.

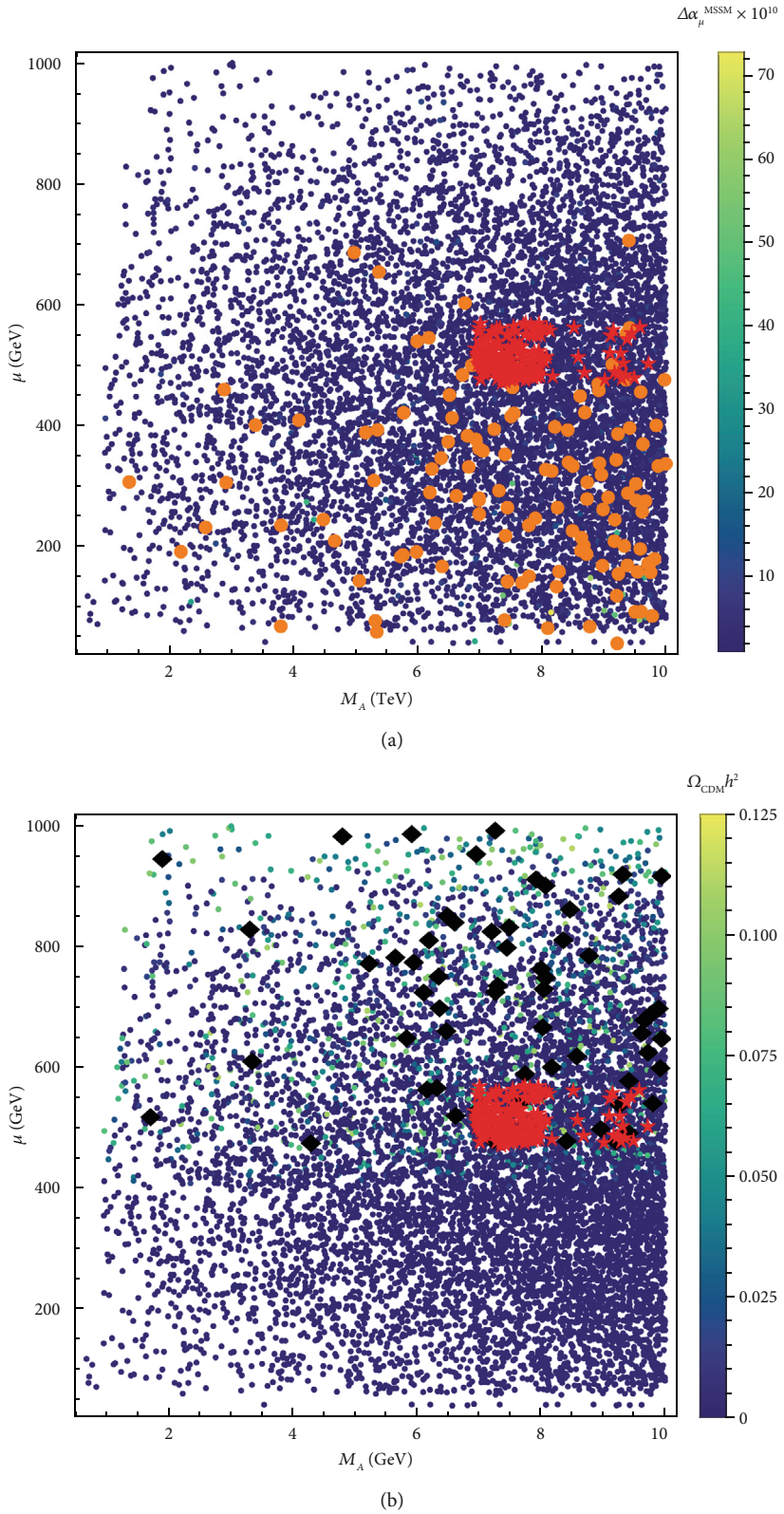

FIGURE 8: The sMSSM predictions for (a) $\Delta\alpha_\mu^{\mathrm{MSSM}}$ and (b) $\Omega_{CDM}h^2$ in the $M_A - \mu$ plane. The color bar indicates their values. Orange points (a) satisfy the 2σ range for $(g-2)_\mu$, black squares (b) fall within the 5σ Planck range for $\Omega_{\mathrm{CDM}}h^2$, and red stars meet both constraints.

TABLE 1: Three benchmark points in the sMSSM that simultaneously satisfy the M_h, M_W, $(g-2)_\mu$, and $\Omega_{\mathrm{CDM}}h^2$ constraints.

Parameter	P_1	P_2	P_3
$m_{0_{1,2}}$	1.774 TeV	2.143 TeV	1.835 TeV
m_{0_3}	14.844 TeV	13.58 TeV	10.317 TeV
$M_{1/2}$	900 GeV	907 GeV	1070 GeV
$\tan\beta$	53.012	54.26 GeV	56.14
A_0	−170.8 GeV	−207 TeV	−209 GeV
M_A	7.41 TeV	9.286 GeV	7.915 TeV
μ	472.9 TeV	477.6 GeV	555 GeV
M_h	125.24 GeV	124.9 GeV	123.63 GeV
M_W	80.397 GeV	80.398	80.398 GeV
$\Delta\alpha_\mu^{\mathrm{MSSM}}$	20.45×10^{-10}	23.08×10^{-10}	20.67×10^{-10}
$\Omega_{\mathrm{CDM}}h^2$	0.119	0.121	0.122

higgsino component decreases. Throughout our entire parameter space, we find that the chargino is the next to LSP (NLSP).

In Figure 7a,b, we display the relative ratio $(m_{\tilde{\chi}_2^0}-m_{\tilde{\chi}_1^0})\times100/m_{\tilde{\chi}_1^0}$ versus $m_{\tilde{\chi}_1^0}$ (μ) while the color bar depicts the value of $\Omega_{\mathrm{CDM}}h^2$. It can be observed that models with neutralinos having less than 20% higgsino component can explain the dark matter relic density. In most of these models, the neutralinos can coannihilate with charginos, resulting in a relic density within the Planck bounds when the mass difference is between 20% and 30%. We find only a few points with a Bino LSP that satisfy the Planck bounds, primarily due to resonances in the annihilation channels $(m_A\sim2\cdot m_\chi)$. From Figure 7, we can also see that achieving $\Omega_{\mathrm{CDM}}h^2$ in the range $0.115<\Omega_{\mathrm{CDM}}h^2<0.125$ requires $m_{\tilde{\chi}_1^0}$ to be greater than 350 GeV and μ to be greater than 450 GeV.

In Figure 8, we present predictions for $\Delta\alpha_\mu^{\mathrm{MSSM}}$ (Figure 8a) and $\Omega_{\mathrm{CDM}}h^2$ (Figure 8b) in the $M_A-\mu$ plane. The color bar indicates the values of $\Delta\alpha_\mu^{\mathrm{MSSM}}$ (Figure 8a) and $\Omega_{\mathrm{CDM}}h^2$ (Figure 8b). The orange points in Figure 8a represent locations where $\Delta\alpha_\mu^{\mathrm{MSSM}}$ falls within the 2σ range required to address the $(g-2)_\mu$ discrepancy, while the black squares in Figure 8b correspond to $\Omega_{\mathrm{CDM}}h^2$ values within the 5σ range of the Planck measurement. The points that simultaneously satisfy $(g-2)_\mu$ and $\Omega_{CDM}h^2$ constraints are shown as red stars. Notably, most of the orange points lie in the region where $\mu\lesssim450$ GeV, whereas most of the black points are situated where $\mu>450$ GeV. This discrepancy makes it challenging to simultaneously account for the $(g-2)_\mu$ discrepancy while adhering to the upper and lower limits of $\Omega_{\mathrm{CDM}}h^2$. The region in which $(g-2)_\mu$ and $\Omega_{\mathrm{CDM}}h^2$ can be satisfied simultaneously is quite narrow, specifically $470\,\mathrm{GeV}\lesssim\mu\lesssim570\,\mathrm{GeV}$ and $7\,\mathrm{Tev}\lesssim M_A$. In Table 1, we present three benchmark points that satisfy M_h, M_W, $(g-2)_\mu$, and $\Omega_{\mathrm{CDM}}h^2$ constraints.

5. Conclusions

The sMSSM is proposed as an alternative model to the CMSSM, which faces challenges in explaining experimental results from the LHC. This model utilizes nonabelian flavor symmetry at the GUT scale to constrain the number of free parameters, requiring only seven in total.

In this paper, we have investigated the predictions for the W boson mass (M_W) and muon's anomalous magnetic moment $(g-2)_\mu$, as well as the dark matter relic abundance $\Omega_{\mathrm{CDM}}h^2$, within the sMSSM. In order to perform the calculations, we generated the SPheno and micrOMEGAs source code for MSSM using Mathematica package SARAH. The SPheno and micrOMEGAs codes were then used in the SSP setup to generate numerical results for the MSSM particle spectra as well as the low energy observables like M_W, $\Delta\alpha_\mu$, and $\Omega_{\mathrm{CDM}}h^2$. For our numerical analysis, we randomly scanned the sMSSM free parameters while respecting the constraints from Higgs boson mass M_h, B-physics observables (BPO), experimental limit on the gluino mass and DM relic density constraints.

The $(g-2)_\mu$ anomaly indicates a preference for lower values of $m_{0_{1,2}}$, setting an upper limit of approximately 3 TeV on this parameter. To satisfy the experimental value of M_h, m_{0_3} needs to exceed approximately 7 TeV, ensuring M_h falls within the range of 123–127 TeV. The Higgs mixing parameter μ was varied from 0 to 2 Tev, but it is constrained by the upper limit on $\Omega_{\mathrm{CDM}}h^2$ to be below 1 TeV, while M_W^{avg} also favors smaller values for μ. The parameter $M_{1/2}$ was explored within the range of 0 – 2 TeV. Experimental constraints on the masses of gluino and scalar quarks require $M_{1/2}$ to exceed 800 GeV, slightly higher than the previously reported lower limit of 700 GeV found in the literature. Additionally, for the sMSSM, achieving $\Omega_{\mathrm{CDM}}h^2$ in the range $0.115<\Omega_{\mathrm{CDM}}h^2<0.125$ necessitates $m_{\tilde{\chi}_1^0}$ and μ to be greater than 350 and 450 GeV, respectively.

In the sMSSM framework, addressing the $(g-2)_\mu$ anomaly prefers μ to be less than 450 GeV, posing challenges in simultaneously satisfying Planck's measurement for $\Omega_{\mathrm{CDM}}h^2$. Our investigations indicate that the $(g-2)_\mu$ discrepancy and the Planck constraints on $\Omega_{\mathrm{CDM}}h^2$ can be met within the sMSSM but though only within a very limited range of the parameter space, specifically $470\,\mathrm{GeV}\lesssim\mu\lesssim570$ GeV and $7\,\mathrm{TeV}\lesssim M_A$.

Data Availability Statement

No new data were created or analyzed in this study. Data sharing is not applicable to this article.

Conflicts of Interest

The authors declare no conflicts of interest.

Funding

The research of M.E.G. is supported by the Spanish Ministerio de Ciencia e Innovacion, under grant PID2022-140440NB-C22.

The research of M.R. is supported by Higher Education Commission, Pakistan, under NRPU grant 20-15867/NRPU/R\&D/HEC/2021.

Acknowledgments

The research of M.E.G. is supported by the Spanish Ministerio de Ciencia e Innovación, under grant PID2022-140440NB-C22. The research of M.R. is supported by Higher Education Commission, Pakistan, under NRPU grant 20-15867/NRPU/R&D/HEC/2021.

References

[1] P. Fayet, "Supergauge Invariant Extension of the Higgs Mechanism and a Model for the Electron and Its Neutrino," *Nuclear Physics B* 90 (1975): 104–124, https://doi.org/10.1016/0550-3213(75)90636-7.

[2] P. Fayet, "Supersymmetry and Weak, Electromagnetic and Strong Interactions," *Physics Letters B* 64, no. 2 (1976): 159–162, https://doi.org/10.1016/0370-2693(76)90319-1.

[3] P. Fayet, "Spontaneously Broken Supersymmetric Theories of Weak, Electromagnetic and Strong Interactions," *Physics Letters B* 69, no. 4 (1977): 489–494, https://doi.org/10.1016/0370-2693(77)90852-8.

[4] H. P. Nilles, "Supersymmetry, Supergravity and Particle Physics," *Physics Reports* 110, no. 1-2 (1984): 1–162, https://doi.org/10.1016/0370-1573(84)90008-5.

[5] H. E. Haber and G. L. Kane, "The Search for Supersymmetry: Probing Physics Beyond the Standard Model," *Physics Reports* 117, no. 2-4 (1985): 75–263, https://doi.org/10.1016/0370-1573(85)90051-1.

[6] R. Barbieri, "Looking Beyond the Standard Model: The Supersymmetric Option," *La Rivista del Nuovo Cimento (1978-1999)* 11, no. 4 (1988): 1–45, https://doi.org/10.1007/BF02725953.

[7] S. L. Glashow, "Partial Symmetries of Weak Interactions," *Nuclear Physics* 22, no. 4 (1961): 579–588, https://doi.org/10.1016/0029-5582(61)90469-2.

[8] S. Weinberg, "A Model of Leptons," *Physical Review Letters* 19, no. 21 (1967): 1264–1266, https://doi.org/10.1103/PhysRevLett.19.1264.

[9] A. Salam, "Weak and Electromagnetic Interactions," *Conf. Proc. C* 680519 (1968): 367–377.

[10] S. L. Glashow, J. Iliopoulos, and L. Maiani, "Weak Interactions With Lepton-Hadron Symmetry," *Physical Review D* 2, no. 7 (1970): 1285–1292, https://doi.org/10.1103/PhysRevD.2.1285.

[11] G. L. Kane, C. F. Kolda, L. Roszkowski, and J. D. Wells, "Study of Constrained Minimal Supersymmetry," *Physical Review D* 49, no. 11 (1994): 6173–6210, https://doi.org/10.1103/PhysRevD.49.6173.

[12] S. Sekmen, "Highlights on Supersymmetry and Exotic Searches at the LHC" https://arxiv.org/abs/2204.03053.

[13] K. S. Babu, I. Gogoladze, S. Raza, and Q. Shafi, "Flavor Symmetry Based MSSM: Theoretical Models and Phenomenological Analysis," *Physical Review D* 90, no. 5 (2014): 056001, https://doi.org/10.1103/PhysRevD.90.056001.

[14] CDF Collaboration, "High-Precision Measurement of the *W* Boson Mass With the CDF II Detector," *Science* 376, no. 6589 (2022): 170–176, https://doi.org/10.1126/science.abk1781.

[15] Particle Data Group, "Review of Particle Physics," *Progress of Theoretical and Experimental Physics* 2022, no. 8 (2022): 083C01, https://doi.org/10.1093/ptep/ptac097.

[16] Muon g-2 Collaboration, "Measurement of the Positive Muon Anomalous Magnetic Moment to 0.20 ppm," *Physical Review Letters* 131, no. 16 (2023): 161802.

[17] Muon g-2 Collaboration, "Measurement of the Positive Muon Anomalous Magnetic Moment to 0.46 ppm," *Physical Review Letters* 126, no. 14 (2021): 141801.

[18] Muon g-2 Collaboration, "Final Report of the Muon E821 Anomalous Magnetic Moment Measurement at BNL," *Physical Review D* 73, no. 7 (2006): 072003, https://doi.org/10.1103/PhysRevD.73.072003.

[19] T. Aoyama, N. Asmussen, M. Benayoun, et al., "The Anomalous Magnetic Moment of the Muon in the Standard Model," *Physics Reports* 887 (2020): 1–166, https://doi.org/10.1016/j.physrep.2020.07.006.

[20] K. S. Babu, I. Gogoladze, Q. Shafi, and C. S. Ün, "Muong−2, 125 GeV Higgs Boson, and Neutralino Dark Matter in a Flavor Symmetry-Based MSSM," *Physical Review D* 90, no. 11 (2014): 116002, https://doi.org/10.1103/PhysRevD.90.116002.

[21] K. S. Babu, I. Gogoladze, and C. S. Un, "Proton Lifetime in Minimal SUSY SU(5) in Light of LHC Results," *Journal of High Energy Physics* 2022, no. 2 (2022): 164, https://doi.org/10.1007/JHEP02(2022)164.

[22] M. Hussain and R. Khalid, "Understanding the Muon Anomalous Magnetic Moment in Light of a Flavor Symmetry-Based Minimal Supersymmetric Standard Model," *Progress of Theoretical and Experimental Physics* 2018, no. 8 (2018): 083B06, https://doi.org/10.1093/ptep/pty087.

[23] E. Bagnaschi, M. Chakraborti, S. Heinemeyer, I. Saha, and G. Weiglein, "Interdependence of the New "MUON G-2" Result and the W-Boson Mass," *European Physical Journal C* 82, no. 5 (2022): 474, https://doi.org/10.1140/epjc/s10052-022-10402-0.

[24] F. Staub, "From Superpotential to Model Files for FeynArts and CalcHep/CompHep," *Computer Physics Communications* 181, no. 6 (2010): 1077–1086, https://doi.org/10.1016/j.cpc.2010.01.011.

[25] F. Staub, "Automatic Calculation of Supersymmetric Renormalization Group Equations and Loop Corrections," *Computer Physics Communications* 182, no. 3 (2011): 808–833, https://doi.org/10.1016/j.cpc.2010.11.030.

[26] F. Staub, "SARAH 3.2: Dirac Gauginos, UFO Output, and More," *Computer Physics Communications* 184, no. 7 (2013): 1792–1809, https://doi.org/10.1016/j.cpc.2013.02.019.

[27] F. Staub, "SARAH 4: A Tool for (Not Only SUSY) Model Builders," *Computer Physics Communications* 185, no. 6 (2014): 1773–1790, https://doi.org/10.1016/j.cpc.2014.02.018.

[28] F. Staub, "Exploring New Models in All Detail With SARAH," *Advances in High Energy Physics* 2015, no. 1 (2015): 840780, https://doi.org/10.1155/2015/840780.

[29] W. Porod, "SPheno, a Program for Calculating Supersymmetric Spectra, SUSY Particle Decays and SUSY Particle Production at e+ e- Colliders," *Computer Physics Communications* 153, no. 2 (2003): 275–315, https://doi.org/10.1016/S0010-4655(03)00222-4.

[30] G. Belanger, F. Boudjema, A. Pukhov, and A. Semenov, "MicrOMEGAs 2.0: A Program to Calculate the Relic Density of Dark Matter in a Generic Model," *Computer Physics Communications* 176, no. 5 (2007): 367–382, https://doi.org/10.1016/j.cpc.2006.11.008.

[31] G. Belanger, F. Boudjema, A. Pukhov, and A. Semenov, "micrOMEGAs_3: A Program for Calculating Dark Matter Observables," *Computer Physics Communications* 185, no. 3 (2014): 960–985, https://doi.org/10.1016/j.cpc.2013.10.016.

[32] D. Barducci, G. Belanger, J. Bernon, et al., "Collider Limits on New Physics Within micrOMEGAs_4.3," *Computer Physics Communications* 222 (2018): 327–338, https://doi.org/10.1016/j.cpc.2017.08.028.

[33] F. Staub, T. Ohl, W. Porod, and C. Speckner, "A Tool Box for Implementing Supersymmetric Models," *Computer Physics Communications* 183, no. 10 (2012): 2165–2206, https://doi.org/10.1016/j.cpc.2012.04.013.

[34] A. H. Chamseddine, R. L. Arnowitt, and P. Nath, "Locally Supersymmetric Grand Unification," *Physical Review Letters* 49, no. 14 (1982): 970–974, https://doi.org/10.1103/PhysRevLett.49.970.

[35] R. Barbieri, S. Ferrara, and C. A. Savoy, "Gauge Models With Spontaneously Broken Local Supersymmetry," *Physics Letters B* 119, no. 4-6 (1982): 343–347, https://doi.org/10.1016/0370-2693(82)90685-2.

[36] L. J. Hall, J. D. Lykken, and S. Weinberg, "Supergravity as the Messenger of Supersymmetry Breaking," *Physical Review D* 27, no. 10 (1983): 2359–2378, https://doi.org/10.1103/PhysRevD.27.2359.

[37] J. de Blas, M. Pierini, L. Reina, and L. Silvestrini, "Impact of the Recent Measurements of the Top-Quark and W-Boson Masses on Electroweak Precision Fits," *Physical Review Letters* 129, no. 27 (2022): 271801, https://doi.org/10.1103/PhysRevLett.129.271801.

[38] C. T. Lu, L. Wu, Y. Wu, and B. Zhu, "Electroweak Precision Fit and New Physics in Light of theWboson Mass," *Physical Review D* 106, no. 3 (2022): 035034, https://doi.org/10.1103/PhysRevD.106.035034.

[39] S. Heinemeyer, W. Hollik, F. Merz, and S. Penaranda, "Electroweak Precision Observables in the MSSM With Nonminimal Flavor Violation," *European Physical Journal C: Particles and Fields* 37, no. 4 (2004): 481–493, https://doi.org/10.1140/epjc/s2004-02006-1.

[40] S. Heinemeyer, W. Hollik, and G. Weiglein, "Electroweak Precision Observables in the Minimal Supersymmetric Standard Model," *Physics Reports* 425, no. 5-6 (2006): 265–368, https://doi.org/10.1016/j.physrep.2005.12.002.

[41] M. E. Gomez, S. Heinemeyer, and M. Rehman, "Effects of Sfermion Mixing Induced by RGE Running in the Minimal Flavor Violating CMSSM," *European Physical Journal C* 75, no. 9 (2015): 434, https://doi.org/10.1140/epjc/s10052-015-3654-8.

[42] S. Heinemeyer and G. Weiglein, "Leading Electroweak Two-Loop Corrections to Precision Observables in the MSSM," *Journal of High Energy Physics* 2002, no. 10 (2002): 072, https://doi.org/10.1088/1126-6708/2002/10/072.

[43] M. Chakraborti, S. Heinemeyer, and I. Saha, "$(g\text{-}2)_\mu$ and Stau Coannihilation: Dark Matter and Collider Analysis," *European Physical Journal C* 84, no. 2 (2024): 165, https://doi.org/10.1140/epjc/s10052-024-12497-z.

[44] S. P. Martin and J. D. Wells, "Muon Anomalous Magnetic Dipole Moment in Supersymmetric Theories," *Physical Review D* 64, no. 3 (2001): 035003, https://doi.org/10.1103/PhysRevD.64.035003.

[45] T. Moroi, "Muon Anomalous Magnetic Dipole Moment in the Minimal Supersymmetric Standard Model," *Physical Review D* 53, no. 11 (1996): 6565–6575, https://doi.org/10.1103/PhysRevD.53.6565.

[46] D. Stockinger, "The Muon Magnetic Moment and Supersymmetry," *Journal of Physics G* 34, no. 2 (2007): R45–R91, https://doi.org/10.1088/0954-3899/34/2/R01.

[47] H. Fargnoli, C. Gnendiger, S. Paßehr, D. Stöckinger, and H. Stöckinger-Kim, "Two-Loop Corrections to the Muon Magnetic Moment From Fermion/Sfermion Loops in the MSSM: Detailed Results," *Journal of High Energy Physics* 2014, no. 2 (2014): 070, https://doi.org/10.1007/JHEP02(2014)070.

[48] G. C. Cho, K. Hagiwara, Y. Matsumoto, and D. Nomura, "The MSSM Confronts the Precision Electroweak Data and the Muon g – 2," *Journal of High Energy Physics* 2011, no. 11 (2011): 068, https://doi.org/10.1007/JHEP11(2011)068.

[49] M. E. Gomez, S. Lola, Q. Shafi, and C. S. Un, "Muong−2and Lepton Flavor Violation in Supersymmetric GUTs," *Physical Review D* 110, no. 9 (2024): 095003, https://doi.org/10.1103/PhysRevD.110.095003.

[50] P. Athron, M. Bach, H. G. Fargnoli, et al., "GM2Calc: Precise MSSM Prediction for (g - 2) of the Muon," *European Physical Journal C* 76, no. 2 (2016): 62, https://doi.org/10.1140/epjc/s10052-015-3870-2.

[51] H. G. Fargnoli, C. Gnendiger, S. Paßehr, D. Stöckinger, and H. Stöckinger-Kim, "Non-Decoupling Two-Loop Corrections to (g−2)μ From Fermion/Sfermion Loops in the MSSM," *Physics Letters B* 726, no. 4-5 (2013): 717–724, https://doi.org/10.1016/j.physletb.2013.09.034.

[52] S. Heinemeyer, D. Stockinger, and G. Weiglein, "Two-Loop SUSY Corrections to the Anomalous Magnetic Moment of the Muon," *Nuclear Physics B* 690, no. 1-2 (2004): 62–80, https://doi.org/10.1016/j.nuclphysb.2004.04.017.

[53] S. Heinemeyer, D. Stockinger, and G. Weiglein, "Electroweak and Supersymmetric Two-Loop Corrections to," *Nuclear Physics B* 699, no. 1-2 (2004): 103–123, https://doi.org/10.1016/j.nuclphysb.2004.08.014.

[54] J. Beuria and A. Dey, "Exploring Charge and Color Breaking Vacuum in Non-Holomorphic MSSM," *Journal of High Energy Physics* 2017, no. 10 (2017): 154, https://doi.org/10.1007/JHEP10(2017)154.

[55] U. Chattopadhyay, D. Das, and S. Mukherjee, "Probing Lepton Flavor Violating Decays in MSSM With Non-Holomorphic Soft Terms," *Journal of High Energy Physics* 2020, no. 6 (2020): 015, https://doi.org/10.1007/JHEP06(2020)015.

[56] P. Slavich, S. Heinemeyer, E. Bagnaschi, et al., "Higgs-Mass Predictions in the MSSM and Beyond," *European Physical Journal C* 81, no. 5 (2021): 450, https://doi.org/10.1140/epjc/s10052-021-09198-2.

[57] LHCb, ATLAS, and CMS Collaborations, *Combination of the ATLAS, CMS and LHCb Results on the* $B^0_{(s)} \longrightarrow \mu^+\mu^-$ *Decays* (LHCb-CONF-2020-002, 2020).

[58] Planck Collaboration, "Planck 2018 Results. VI. Cosmological Parameters," *Astronomy & Astrophysics* 641 (2020)A6 [erratum: Astron. Astrophys. 652 (2021), C4].